

1 **Early detection of undesirable deviations in must fermentation using a** 2 **portable FTIR-ATR device and multivariate analysis**

3 Julieta Cavaglia¹ | Barbara Giussani² | Montserrat Mestres¹ | Miquel Puxeu³ | Olga Busto¹ | Joan Ferré⁴ | Ricard Boqué⁴
4 ¹Department of Analytical Chemistry and Organic Chemistry, Universitat Rovira I Virgili, iSens Group, Campus
5 Sescelades, 43007 Tarragona, Spain
6 ²Università degli Studi dell'Insubria, Dipartimento di Scienza e Alta Tecnologia, Via Valleggio 9, 22100 Como, Italy
7 ³Wine Technology Park (VITEC), Falset, Tarragona, Spain
8 ⁴Department of Analytical Chemistry and Organic Chemistry, Universitat Rovira I Virgili, Chemometrics, Qualimetrics
9 and Nanosensors Group, Campus Sescelades, 43007 Tarragona, Spain
10

11 **Summary**

12 A portable FTIR-ATR spectrometer was used to monitor small-scale must fermentations
13 (microvinifications) with the aims to describe the process and to early detect problematic
14 fermentations. Twenty fermentations at normal operation conditions (NOC) and 3
15 fermentations that were intentionally deviated from NOC (yeast assimilable nitrogen
16 deficiency - YAN) were monitored. FTIR-ATR spectra were registered after a minimum
17 sample pretreatment during the fermentation process. In addition, density, sugars (glucose
18 and fructose) and acetic acid contents were determined by traditional methods. Different
19 multivariate analysis strategies (global and local models) were applied to the
20 spectroscopic data to describe the evolution of the NOC fermentation and to early detect
21 the abnormal fermentations. Global models based on principal component analysis (PCA)
22 and partial least squares discriminant analysis (PLS-DA) allowed to describe the
23 fermentations evolution in time and to correctly classify NOC and YAN fermentations.
24 Abnormal deviations were successfully detected by developing one model for each
25 sampling time. YAN experiments could be identified 49 hours after the beginning of the
26 fermentations by means of Hotelling T^2 and residual F statistics. In conclusion, ATR-
27 FTIR coupled to multivariate analysis showed great potential as a fast and simple at-line
28 analysis tool to monitor wine fermentation and to early detect fermentation problems

29 **Key words:** ATR-FTIR, fermentation monitoring, multivariate analysis, wine

30 **Introduction**

31 In the winemaking industry, the control of the whole production chain, from harvest to
32 bottling, is essential to obtain high-quality wines. One of the crucial phases in wine
33 production is certainly the must fermentation, which is the biological transformation of
34 grape juice into wine. Whereas it comprises many biochemical reactions, the most
35 important change is the conversion of sugars into ethanol and CO₂. Nevertheless,
36 the secondary reactions that take place during must fermentation have a substantial
37 impact on the quality, flavor and character of the final wine.¹

38 Must fermentation requires, therefore, a thorough monitoring: failing to achieve a
39 successful process control at this stage may result in stuck or sluggish fermentations that
40 could throw away a whole vintage or lead to low quality wines.²

41 Several routine measurements such as density, temperature and pH, are usually carried
42 out throughout the fermentation process in wine cellars. However, additional
43 measurements (e.g. total and volatile acidity, sugars, SO₂, assimilable nitrogen) which are
44 often costly, time-consuming and require specific equipment and personnel, are
45 commonly performed to gain more information.³

46 In 2004 the United States Food and Drug Administration introduced the concept of
47 'Process Analytical Technologies' (PAT), aiming at implementing a real-time monitoring
48 system through the production chain. This would replace final product testing as quality
49 is controlled during the production process, giving the possibility to 'readjust' a process
50 before the product is made and thus minimizing rejects.⁴

51 Over the last decades, infrared spectroscopy, in combination with multivariate analysis,
52 has proven to be a powerful tool for food analyses and, specifically, for wine analyses.
53 Partial Least Squares Regression (PLSR) has been the most used calibration algorithm to
54 predict chemical or physical parameters in wine from spectroscopic data.⁵

55 As reviewed by dos Santos et al., it has been shown that Near Infrared Spectroscopy (NIR)
56 and Mid Infrared Spectroscopy (MIR) are both suitable techniques to predict several
57 quality control parameters in grape juice, must and wine at different production stages,
58 including total sugars (mainly glucose and fructose), ethanol, glycerol, total phenolics,
59 anthocyanins or acetic acid, among other compounds.⁶ The potential of NIR and MIR to
60 monitor and model alcoholic fermentations was also investigated, demonstrating the
61 usefulness of these techniques to monitor the evolution of the fermentation process.⁷⁻¹⁰
62 Regmi et al used MIR in the transmission mode with PLSR to predict the concentration
63 of several acids in wine. They obtained good calibration results for citric, malic, tartaric,
64 acetic, succinic, and lactic acids.¹¹ Moreover, MIR spectroscopy with PLS regression was
65 also used for the quantification of reducing sugars, titrable acidity, total soluble solids,
66 pH, and some phenolic compounds (see the review by Damberg et al and references
67 therein¹²)
68 Among the different vibrational spectroscopic modes, the attenuated total reflectance
69 MIR (ATR-MIR) mode is particularly advantageous over traditional transmission MIR
70 modes because it requires little or even no sample pretreatment and it is faster and simpler
71 to use. Moreover, as the infrared beam only penetrates the samples a few microns, so
72 typical spectra saturation due to the high-water absorption band does not occur.¹³
73 ATR-MIR was successfully employed to determine the total soluble solids (°Brix), pH,
74 total phenolics, ammonia, free amino nitrogen, and yeast assimilable nitrogen (YAN) in
75 grape juice samples.¹⁴ Kim *et al.* were able to predict alcohol, reducing sugars and
76 titratable acidity in fermenting samples of Makgeolli rice wine using ATR-MIR, thus
77 proving the suitability of this technique to monitor the fermentation process.¹⁵ Wu et al
78 used ATR-MIR to successfully monitor the course of Chinese rice wine fermentation.¹⁶

79 The researchers were capable to predict total sugar, ethanol, titratable acidity, and amino
80 nitrogen by applying different calibration models. Previously, Cozzolino et al had also
81 investigated the suitability of ATR-MIR to predict the time course of fermentation in
82 samples at different days of fermentation using PLS discriminant analysis (PLS-DA)
83 models. They obtained promising results, with low standard errors of prediction.¹⁷
84 Portable FTIR instruments are rapidly gaining popularity across the food industry sector.
85 They are cheaper, simpler to use, and faster than traditional instruments and allow sample
86 analysis to be performed directly on the field: for these reasons, they could be considered
87 powerful tools to rapidly perform quality control test and process monitoring especially
88 when coupled with multivariate analysis. Portable FTIR instruments have been used for
89 multiple purposes in foodstuff analysis, including, eg, the prediction of fatty acid content
90 in marine oil, quantification of acrylamide in potato chips, or quantification of trans-fat
91 content in fat and oil samples.¹⁸⁻²⁰ To our knowledge, this is the first time that a portable
92 ATR-FTIR device is used for the analysis of must and wine fermenting samples.
93 The aim of this research was to develop a strategy to monitor the must fermentation and
94 to early detect deviation from the typical fermentation using a portable ATR-FTIR
95 instrument coupled with multivariate analysis. The first step of the study concerned the
96 investigation of the suitability of the instrument to the scope. Twenty-three must
97 fermentations were carried out, and data were recorded during the whole process after a
98 minimum sample pretreatment. Different multivariate approaches were applied for
99 modeling the typical fermentation process, thus describing the normal operation
100 conditions (NOC), and to early predict deviation from the NOC, in particular for a
101 fermentation run with deficiency of assimilable nitrogen. The choice of the chemometric
102 strategy was driven by the idea to give to winemakers a quite easy to understand process
103 control model, which coupled with a portable device resulted in a process control

104 methodology cheap and easy to implement.

105

106 **Material and methods**

107 *Samples*

108 Concentrated white natural must was obtained from “Concentrats Pallejà” (Riudoms,
109 Spain). This was diluted 1:4 with distilled water to give an initial sugar (glucose and
110 fructose) concentration of about 200 g/L (to emulate the concentration of sugars found in
111 a must coming from optimal mature grapes) and supplemented with 0.3 g/L of
112 actimaxbio*(Agrovin) to ensure a YAN source. Table 1 summarizes the chemical
113 parameters of must once diluted and supplemented.

114

209 g/L glucose + fructose

228 g/L yeast assimilable nitrogen

pH = 3.94

Total Acidity = 7.0 g Tartaric acid/L

Density = 1.0865 g/mL

Malic acid = 2.12 g/L

115 **Table 1.** Chemical Parameters of diluted must

116

117 The microvinifications were conducted in 500 mL Erlenmeyer flasks containing 350 mL
118 of diluted must and under constant temperature of 18°C. Twenty microvinifications were
119 carried out without manipulating them or varying any parameter (NOC). Moreover, three
120 microvinifications were intentionally altered to promote nitrogen deficiency: they were
121 run without the addition of the YAN source.

122 *Yeast and nutrients*

123 The alcoholic fermentations were carried out by *Saccharomyces cerevisiae* yeast, and the
124 inoculation was done as follows: 3.15 g of active dry yeast “VitilevureDV10” (Danstar

125 Ferment AG, Denmark) was rehydrated in 60 mL of milliQ water, and 2 mL of yeast
126 solution was added to the 23 Erlenmeyer flasks containing 350 mL of must, to reach a
127 final concentration of 0.3 g/L in each flask.

128 *ATR-FTIR spectroscopic analysis*

129 Data acquisition was performed using a portable 4100 ExoScan FTIR instrument
130 (Agilent, California, USA), equipped with an interchangeable spherical ATR sampling
131 interface, consisting on a diamond crystal window.

132 A total of 17 sampling points (times) were analyzed before the end of fermentation.
133 Samples were randomly collected twice a day (every 12 hours approximately),
134 centrifuged at 10 000 rpm for 10 minutes so that the supernatant could be collected using
135 a micropipette. A drop of the supernatant was placed on top of the crystal using a Pasteur
136 pipette, ensuring that the surface was completely covered with the sample, and the
137 spectrum was recorded immediately afterwards. All spectra were recorded in the region
138 of 3999 to 649 cm, with 32 scans and 8 cm⁻¹ resolution. An air background was collected
139 after every triplicate, that is, one background per sample. After each measurement, the
140 crystal was carefully cleaned using deionized water and cotton wipes. Spectra were
141 examined using the Microlab PC software (Agilent, California, USA), and data were
142 saved as .spc files.

143 Absorbance data were used for the chemometric calculation. The mean of the sample
144 replicates was calculated, and different preprocessing (smoothing and normalization)
145 methods were tested in order to remove unwanted variations not due to changes in
146 chemical compounds during fermentation, such as baseline drifts and noise observed in
147 the raw spectra.

148 The final data was a three-way array containing the spectroscopic signals of 23 samples
149 (20 NOC and three YAN) with 899 wavelengths recorded for 17 times covering a total of
150 258 hours of fermentation.

151 *Quality Control Parameters*

152 Reference analyses were carried out every 24 hours to monitor the fermentation process.
153 Density was measured using an Densito 30PX electronic densimeter (Mettler Toledo),
154 whereas sugars (glucose and fructose) and acetic acid were determined using a Y15
155 Analyser (Biosystems, Barcelona, Spain). All the analyses were performed right after
156 sample collection.

157 *Multivariate Analysis*

158 The collected data consisted of a three-way structure containing spectra ($J = 899$), batches
159 or samples ($I = 23$), and sampling times ($K = 17$). Depending on the information we want
160 to obtain, this data matrix can be treated as a multiway structure, unfolded into a two-way
161 structure or divided into several matrices, usually one for each sampling time. Unfolding
162 can be performed in several ways, depending on the mode that is kept in common. If
163 unfolding is performed sample-wise, the final matrix has dimensions ($I \times KJ$), with each
164 row containing the spectra of a given sample at the different time points. If the spectral
165 mode is common, then the final unfolded matrix has dimensions ($J \times IK$). In this last
166 matrix, each row contains a spectrum of sample i at time point k . Finally, if unfolding is
167 performed timewise, the final matrix has dimensions ($K \times JI$), where each row contains the
168 spectra of all samples at time point k . Once unfolded, the matrix structure can be
169 processed also in different ways. Global approaches can be applied, which means that all
170 the data collected throughout the process are used in a global model. Alternatively, local
171 approaches refer to the use of data separately from each sampling time to build
172 independent models.²¹ Principal component analysis (PCA), partial least squares

173 regression (PLSR), and PLS-DA were used to process the data. The strategies used in this
174 work are described in the following section.

175 All the models were cross-validated with random subsets (10 splits and five iterations).

176 In PLSR and in PLS-DA, the root mean square error of cross-validation (RMSECV) error
177 was used to estimate the optimum number of latent variables to be used in prediction.

178 All multivariate data analyses were performed using the PLS Toolbox v8.6.1
179 (Eigenvector Research Inc., Eagan, USA) with MATLAB R2015b (The MathWorks,
180 Natick, USA).

181

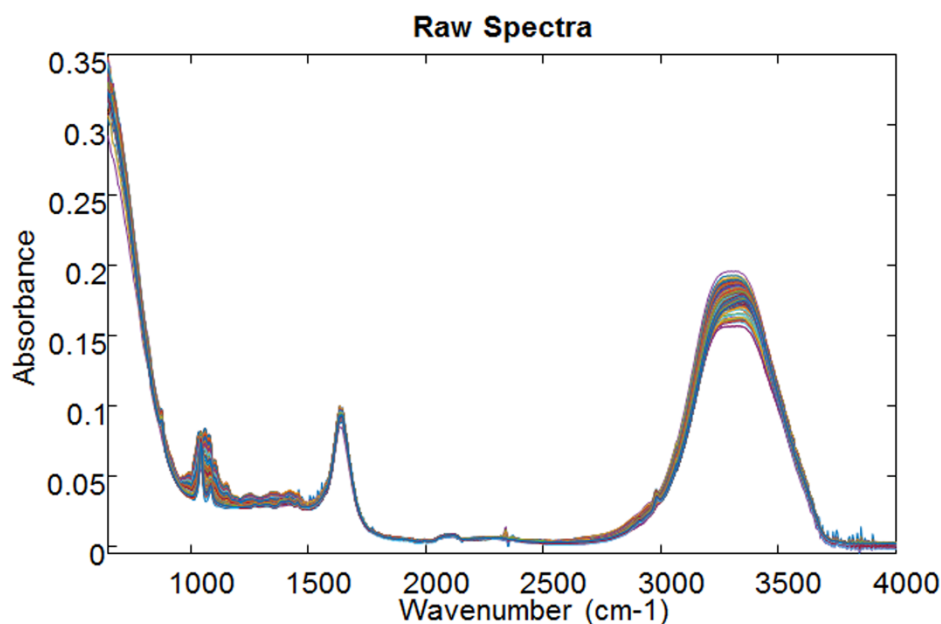
182 **Results and discussion**

183 *Spectroscopic Data*

184 Firstly, the signal quality was investigated. Several combinations of spectral resolution
185 and number of acquisition scans were tested. An increase in the resolution (8-4-2 cm^{-1}
186 was tested) did not add any relevant information to the spectra: peaks were well described,
187 and this was confirmed by the chemometric modeling, which did not change in
188 performances when using spectra recorded at higher resolution values. Regarding data
189 acquisition, scan numbers from 32 to 512 were tested, but the final models did not change
190 relevantly in their performances. For this reason, a more rapid solution (32 scans) was
191 preferred as it allowed reaching satisfactory results.

192 The evolution of the ATR-FTIR spectra throughout the whole fermentation process is
193 shown in Figure 1. Due to the high absorbance of the O-H bond of water in the mid-
194 infrared region and the high amount of overlapping vibrational modes in similar
195 molecules, single molecules peak assignment is quite difficult. The main changes in the
196 spectra are found between 950-1500 cm^{-1} and 3000-3500 cm^{-1} . The bonds in the 950-
197 1500 cm^{-1} region could be associated with sugars and organic acids. Peaks between 1500

198 and 1200 cm^{-1} correspond mainly to deformations of $-\text{CH}_2$, deformations of $\text{C}-\text{C}-\text{H}$ and
199 $\text{H}-\text{C}-\text{O}$. On the other hand, peaks between 1200 and 950 cm^{-1} could be related to
200 stretching modes of $\text{C}-\text{C}$ and $\text{C}-\text{O}$. The broad band between 3000 and 3500 cm^{-1} could
201 be ascribed to water and ethanol $\text{O}-\text{H}$ stretching vibrations. These results are in agreement
202 with the literature, both in ATR and transmission IR modes²².



203
204 **Figure 1.** FTIR full spectra for all the fermenting samples (including all time points).

205 *Data preprocessing*

206 After calculation of the mean of the sample replicates, different preprocessing methods
207 were tested to overcome baseline drifts and noise observed in the raw spectra. The
208 following combination of preprocessing methods gave the best results:

- 209 - Smoothing (Savitzky-Golay) filter: window size 11pts, polynomial order 2.
- 210 - Standard Normal Variate (SNV) normalization
- 211 - Mean Centering

212 Because the objective of the work was to detect deviations from the NOC, the average
213 trajectory of each variable was subtracted in the batches. In this way, models focused the
214 attention on the variability around these trajectories.

215 *Fermentation control parameters*

216 Density, sugars (glucose and fructose) and acetic acid values during fermentation are
217 depicted in Figure 2, in which NOC samples are described by circles and YAN samples
218 are indicated with stars. Density vary between 1,09 g/mL at the beginning of the
219 fermentation and 0,99 at the end of the process, showing typical values for white wine
220 fermentations. NOC samples reached sugar depletion sooner than nitrogen-deficient
221 samples. This behaviour could be explained considering that a lack of nutrients causes a
222 decrease in yeast's enzymatic activity, which results in sluggish fermentations². A higher
223 production of acetic acid could be observed in the nutrient deficient samples. Acetic acid

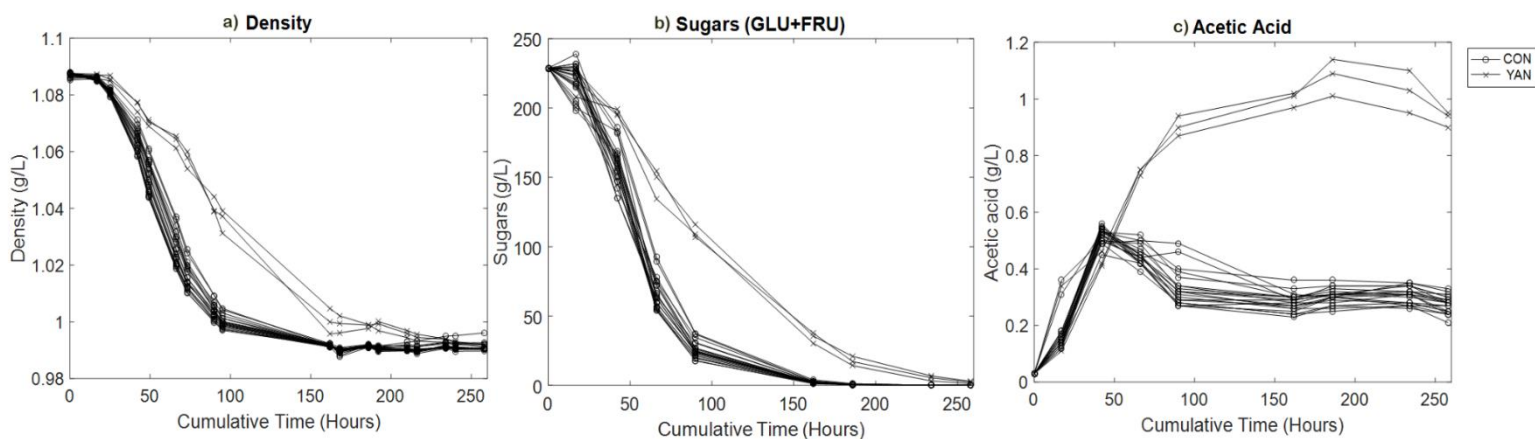


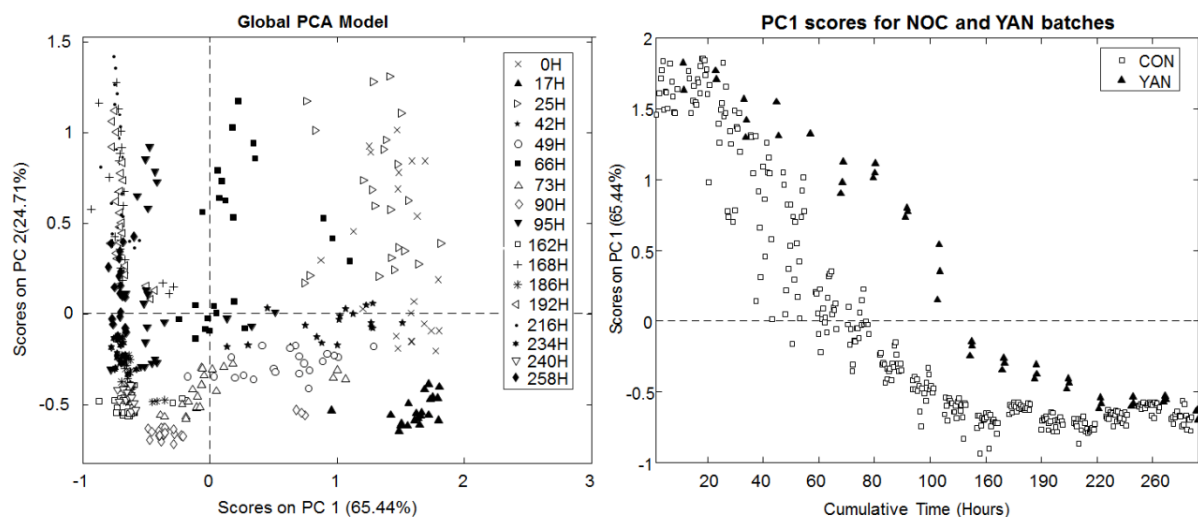
Figure 2. Evolution of chemical parameters: A: Density; B: Sugars (Glucose+Fructose); and C: Acetic acid.

224 is a by-product of yeast metabolism, which is generated from acetyl-coenzyme A derived
225 from oxidative decarboxylation of pyruvate²³. An increase of its values could be often
226 observed in stuck fermentations, where conditions for yeast development are not
227 optimal.²⁴

228 *Global PCA model*

229 First, we decided to explore the whole data set following a global approach. Data
230 collected from NOC experiments were arranged in a two-way unfolded matrix with
231 samples \times times in the rows and spectra (wavenumbers) in the columns, with the aim to

232 study the sample evolution throughout the fermentation process. The final matrix had size
 233 391×899 . The score plot for the first two PCs (90.16% of the total variance) is reported
 234 in Figure 3. A trend in the samples position clearly emerges from the graph: samples are
 235 located along the first PC, from positive to negative values, according to the sampling
 236 time. All the NOC experiments and the YAN experiments showed a similar trend. While
 237 the PC1 accounted for the spectra variation in time, the second PC seemed to account for
 238 an experimental variability that could be possibly related to small differences between the
 239 evolving of samples during the fermentation process. Focusing the attention on PC1, the
 240 scores showed a tendency very similar to the one described for density and sugar values,
 241 confirming that this component mainly explains the fermentation evolution in time.
 242 Moreover, it is possible to distinguish the NOC and YAN fermentations that show a
 243 similar but not identical behavior. This model was able to detect the main changes in the
 244 samples at the different sampling times. This first promising result motivated us to further
 245 investigate the possibility to use the portable ATR-FTIR instrument to monitor the wine
 246 fermentation process.

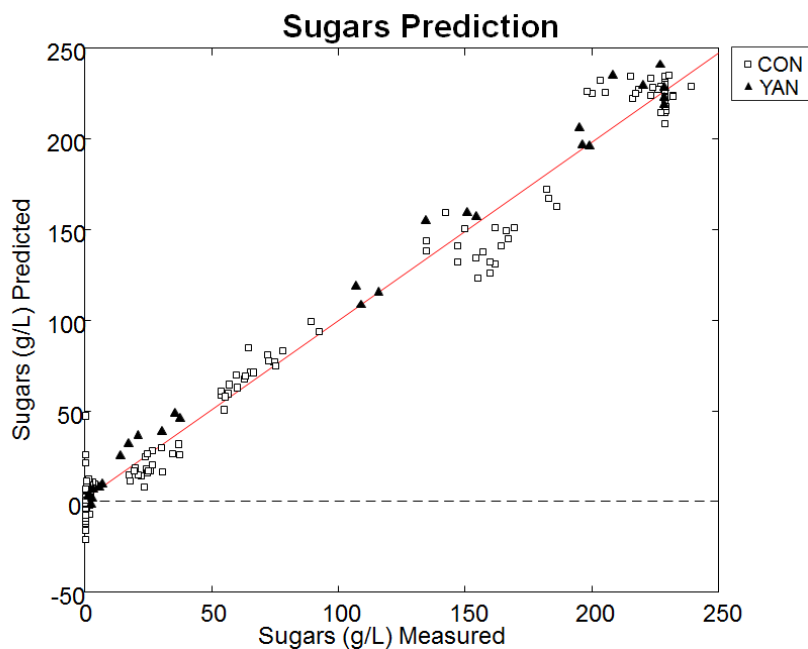


247

248

249 **Figure 3.** Scores plot for the global PCA model (left), samples are marked according to their sampling time. PC1 scores for NOC and YAN batches (right).

250 A partial least squares (PLS) regression model was then built on the same unfolded data
 251 matrix to predict the total sugars (glucose and fructose) concentration values from the
 252 recorded ATR-FTIR spectra along the fermentation. The values obtained with the
 253 reference analytical method were used as the Y data. The aim of this model was to prove
 254 the suitability of the portable ATR-FTIR spectrometer to monitor the wine fermentation
 255 through the prediction of one of the most important parameters, that is, the change in the
 256 total sugar content along fermentation. The statistical parameters of the regression model
 257 (two factors accounting the 98.68% of the Y variability) were RMSEC = 10.6 g/L,
 258 RMESCV = 10.9 g/L, $R^2 = 0.987$, and bias = -0.02 g/L
 259 Figure 4 shows the measured vs PLSR predicted total sugar. There is a good agreement
 260 between measured and predicted values, confirming that coupling ATR-FTIR portable
 261 spectroscopy and multivariate analysis allowed to successfully monitor one of the major
 262 changes in fermenting wine samples and possibly the whole fermentation process.



263
 264 **Figure 4.** Measured vs Predicted concentrations of sugars (glucose+fructose).

265 *Global PLS-DA model*

266 The global data analysis strategy was then employed with the aim of evaluate the
267 possibility to distinguish NOC fermentation from YAN fermentation using the spectra
268 collected with the portable device during the whole fermentation process. In this case, the
269 original three-way data matrix was unfolded in a time-wise manner so that sample
270 direction was maintained. The unfolded matrix size was 23x15283 (23 samples x (899
271 variables x 17 time points)). A PLS-DA strategy was chosen due to the small number of
272 samples and a PLS-DA model was built in order to classify fermentation experiments in
273 NOC and YAN classes (in the Y vector, zeros were attributed to the NOC class samples,
274 and ones were attributed to YAN class samples)

275 Figure 5 depicts the classification between normal and nitrogen deficient fermentations.
276 As emerged from the graph, the two classes are well separated and no overlapping
277 between them could be observed. The threshold used to discriminate between the classes
278 was calculated as the value that best splits the classes with the least probability of both
279 false positives and false negatives (assuming that the predicted values for each class are
280 approximately normally distributed). The algorithm is implemented in the PLS-Toolbox.
281 Even if the number of YAN fermentation experiments is quite small with respect to the
282 NOC fermentation, these results are really promising, showing the possibility to
283 distinguish the different types of fermentation when spectra collected along all the
284 fermentation process are available.

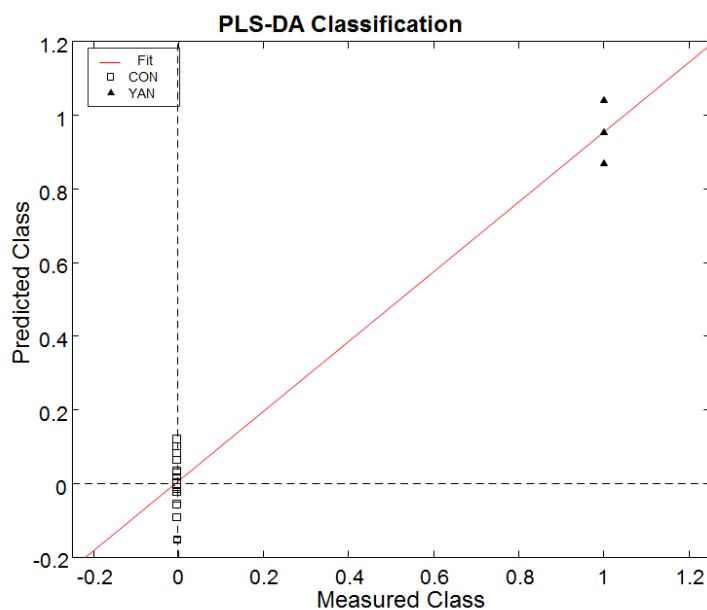


Figure 5. PLS-DA model for control (CON) and nutrient deficient samples (YAN). Zero was assigned to CON samples whereas ones was used for YAN samples.

285

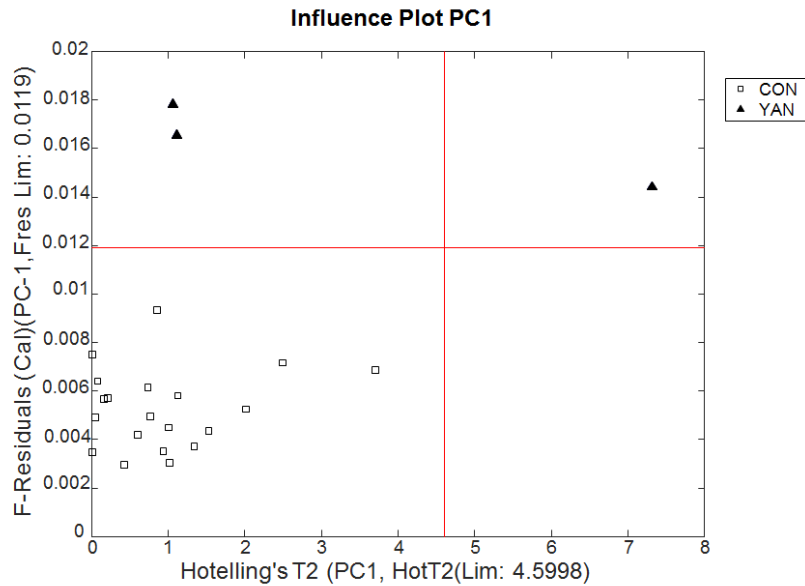
286

287 *k-PCA (Local Models)*

288 A local strategy to early predict deviations from NOC was then developed. Local k-PCA models
 289 were built using the two-way matrices (samples \times wavelengths [23 \times 899]) obtained separately
 290 for each sampling time collected (a total of 17 data matrices, one for each time). A very
 291 satisfactory result was obtained, as the model built with spectra recorded after 49 hours
 292 (time point 4) was able to distinguish between NOC and YAN fermentations processes.
 293 Figure 6 shows the influence plot for PC1. The same result was obtained with the PLS-
 294 DA modeling strategy as expected. Several PLS-DA models were built, one for each
 295 sampling time. The PLS-DA model built after 49 hours (time point 4) gave the 100% of
 296 correct classification with no overlap between the classes (0 was attributed to NOC class,
 297 1 was attributed to YAN class).

298 Using a moving window approach (see the article by Camacho et al and references
 299 therein²¹) to try to perform an earlier prediction of the deviation from NOC did not
 300 provide better results. A possible explanation to this behavior could be the quite small
 301 number of sampling points analyzed at the beginning of the fermentation, which is

302 clearly the moment of the whole process in which the main changes (especially in
 303 abnormal fermentations) occurred. For this reason, any other evolving modeling
 304 approach was not considered in this first step of the research project



305 **Figure 6.** Influence plot for the k-PCA model at time point 4.
 306

307 *Biological process time*

308 To monitor the evolution of the abnormal YAN fermentation, the approach developed by
 309 Jørgensen et al. was applied²⁵. The reasoning behind the method is that each fermentation,
 310 starting similar initial conditions, can evolve slower or faster, and this different behavior
 311 can be detected. The idea is that spectra of the NOC samples can be modelled against the
 312 evolving time, but if this relationship is different for the abnormal batches then it means
 313 the fermentation has a different speed or has followed another direction. The method
 314 operates as follows:

- 315 1) The original data structure is unfolded keeping as common the spectral mode.
 316 Then, the relative times of all fermentations of all NOC samples are calculated, as
 317 the real time at time point k divided by the total time of the fermentation:

318
$$\text{Rel time}_{fermi} = \frac{\text{Actual time}_{fermi}}{\text{Total time}_{fermi}}$$

319 The final time of a fermentation is assumed to have a relative time of 1, and the
320 rest of relative times take values within 0 and 1. The relative time is also the % of
321 evolution of the fermentation (relative time 0.6 means the fermentation is at 60%).
322 Finally, a PLS regression model is built between the spectra of all NOC samples
323 against the relative times. At this point, it is important to decide what the total
324 time of a fermentation is. We decided to use the time where the sugar value was
325 around the detection limit of the instrument, what coincided with the usual glucose
326 value of a wine at the end of the fermentation process.

327

- 328 2) The spectra of all NOC samples at all fermentation times are regressed onto the
329 previous PLS model to estimate what is called the “biological” process time. This
330 is done because the assumption is that the difference between relative and
331 biological time is due to the fermentation process.
- 332 3) A second PLS model is built between the NOC spectra and the “biological” time,
333 that is, the predicted time of the first PLS model.
- 334 4) From this second PLS model, the resulting scores are used to build control charts
335 for future batches. In these control charts (one for each PLS factor) confidence
336 limits are calculated from the NOC training set (± 2 and $3\pm$ standard deviation
337 curves) and represented *vs* “biological” time (see Fig 7).
- 338 5) Finally, to monitor future batches, their spectra are used in the second PLS model
339 to predict the scores and the biological process time. Both predicted biological
340 process time and scores are used in the control chart evaluations (see Fig 7). This
341 allows on-line monitoring of batch evolution.

342 The approach was applied to monitor both normal control samples (NOC) and the YAN
343 abnormal samples. Results are shown in Figure 7. It can be seen that YAN samples evolve

344 in a substantially slower way, but the relationship between the spectra and time works.

345 The prediction of the biological time for the YAN sample confirms that, when the NOC

346 samples are 100% fermented, YAN samples are about 60% fermented.

347

348 **Conclusions**

349 Monitoring the fermentation process is a crucial step in order to obtain high-quality wines

350 and avoid materials and money waste. Several analytical techniques measuring a variety

351 of analytes and properties fit for the purpose and give good performances, but often they

352 need intensive sample preparation, or highly specialized instruments and operators,

353 besides costly and time-consuming analyses. This work was focused on the use of a

354 portable, easy-to-use ATR-MIR device, coupled with multivariate analysis, as a rapid and

355 economical strategy to monitor fermentation processes and to detect deviation from NOC.

356 The results obtained were very satisfactory. The prediction of the sugar content in

357 fermenting samples from the beginning to the end of fermentation was performed,

358 demonstrating the possibility to use this portable device to rapidly monitor fermentations

359 running under normal operation condition. Moreover, slower fermentations (YAN) could

360 be detected at an early stage of fermentation (when NOC are well described), giving the

361 possibility to the winemaker to eventually correct the process and to obtain a good quality

362 product.

363 Future work will be done increasing the number of samples both in NOC and in abnormal

364 operation conditions, especially at the beginning of the fermentation, as it emerged from

365 the models that the first 50 hours of fermentation are possibly the crucial ones to detect

366 deviations from NOC conditions. We will take advantage of other strategies (eg, time

367 evolving and moving average) to develop multivariate models. Moreover, a chemometric

368 strategy will be developed to compare fermentations running in different times, for

369 different wine types and including other problems that may occur during the fermentation
370 process.

371 **Acknowledgments**

372 We thank the Spanish Ministry of Economy and Competitiveness (project AGL2015-
373 70106-R) for financial support and AGAUR (Generalitat de Catalunya) for awarding the
374 FI grant (2018 FI_B 00844) to Julieta Cavaglia.

375

376 **References**

- 377 1. Ciani M, Comitini F, Mannazzu I. In: Jørgensen SE, Fath BD, eds. Encyclopedia of
378 Ecology. Oxford, UK: Elsevier B.V.; 2008:1548-
379 1557. <https://doi.org/10.1093/aob/mcp308>.
- 380 2. Bisson LF. Stuck and sluggish fermentations. *Am J Enol Vitic.* 1999;50:107-119.
- 381 3. Ribéreau-Gayon P, Dubourdieu D, Donèche B, Lonvaud A. Handbook of Enology
382 Volume 1 The Microbiology of Wine and Vinifications. 2nd ed. Chichester, UK: John
383 Wiley & Sons Ltd; 2006. <https://doi.org/10.1002/0470010363.fmatter>.
- 384 4. Van Den Berg F, Lyndgaard CB, Sørensen KM, Engelsen SB. Process analytical
385 technology in the food industry *. *Trends Food Sci Technol.* 2013;31(1):27-35.
- 386 5. Bauer R, Bauer FF, Kossmann J, Koch KR, Esbensen KH. FTIR spectroscopy for
387 grape and wine analysis. *Anal Chem.* 2008;80(5):1371-1379.
- 388 6. dos Santos CAT, Páscoa RNMJ, Lopes JA. A review on the application of vibrational
389 spectroscopy in the wine industry: from soil to bottle. *Trends Anal Chem.* 2017;88:100-
390 118.
- 391 7. Di Egidio V, Sinelli N, Giovanelli G, Moles A, Casiraghi E. NIR and MIR
392 spectroscopy as rapid methods to monitor red wine fermentation. *Eur Food Res*
393 *Technol.* 2010;230(6):947-955.
- 394 8. Urtubia A, Pérez-Correa JR, Pizarro F, Agosin E. Exploring the applicability of MIR
395 spectroscopy to detect early indications of wine fermentation problems. *Food Control.*
396 2008;19(4):382-388.
- 397 9. Buratti S, Ballabio D, Giovanelli G, et al. Monitoring of alcoholic fermentation using
398 near infrared and mid infrared spectroscopies combined with electronic nose and
399 electronic tongue. *Anal Chim Acta.* 2011;697(1-2):67-74.

- 400 10. Emparán M, Simpson R, Almonacid S, Teixeira A, Urtubia A. Early recognition of
401 problematic wine fermentations through multivariate data analyses. *Food Control*.
402 2012;27(1):248-253.
- 403 11. Regmi U, Palma M, Barroso CG. Direct determination of organic acids in wine and
404 wine-derived products by Fourier transform infrared (FT-IR) spectroscopy and
405 chemometric techniques. *Anal Chim Acta*. 2011;732:137-144.
- 406 12. Damberg R, Gishen M, Cozzolino D. A review of the state of the art, limitations, and
407 perspectives of infrared spectroscopy for the analysis of wine grapes, must, and
408 grapevine tissue. *Appl Spectrosc Rev*. 2015;50(3):261-278.
- 409 13. Craig AP, Franca AS, Irudayaraj J. *High Throughput Screening for Food Safety*
410 *Assessment*. Amsterdam, The Netherlands: Elsevier Ltd; 2015:165-
411 194. <https://doi.org/10.1016/B978-0-85709-801-6.00007-1>.
- 412 14. Shah N, Cynkar W, Smith P, Cozzolino D. Use of attenuated total reflectance
413 midinfrared for rapid and real-time analysis of compositional parameters in
414 commercial white grape juice. *J Agric Food Chem*. 2010;58(6):3279-3283.
- 415 15. Kim DY, Cho BK, Lee SH, Kwon K, Park ES, Lee WH. Application of Fourier
416 transform-mid infrared reflectance spectroscopy for monitoring Korean traditional
417 rice wine 'Makgeolli' fermentation. *Sens Actuators B*. 2016;230:753-760.1
- 418 16. Wu Z, Xu E, Long J, et al. Monitoring of fermentation process parameters of Chinese
419 rice wine using attenuated total reflectance mid-infrared spectroscopy. *Food Control*.
420 2015;50:405-412.
- 421 17. Cozzolino D, Curtin C. The use of attenuated total reflectance as tool to monitor the
422 time course of fermentation in wild ferments. *Food Control*. 2012;26(2):241-246.

- 423 18. Ayvaz H, Rodriguez-Saona LE. Application of handheld and portable spectrometers
424 for screening acrylamide content in commercial potato chips. *Food Chem.*
425 2015;174:154-162.
- 426 19. Karunathilaka SR, Mossoba MM, Chung JK, Haile EA, Srigley CT. Rapid prediction
427 of fatty acid content in marine oil omega-3 dietary supplements using a portable Fourier
428 transform infrared (FTIR) device & partial least-squares regression (PLSR) analysis. *J*
429 *Agric Food Chem.* 2017;65(1):224-233.
- 430 20. Mossoba MM, Kramer JKG, Azizian H, et al. Application of a novel, heated, nine-
431 reflection ATR crystal and a portable FTIR spectrometer to the rapid determination of
432 total trans fat. *J Am Oil Chem Soc.* 2012;89(3):419-429.
- 433 21. Camacho J, Picó J, Ferrer A. The best approaches in the on-line monitoring of batch
434 processes based on PCA: does the modelling structure matter? *Anal Chim Acta.*
435 2009;642(1-2):59-68.
- 436 22. Cozzolino D, Cynkar W, Shah N, Smith P. Feasibility study on the use of attenuated
437 total reflectance mid-infrared for analysis of compositional parameters in wine. *Food*
438 *Res Int.* 2011;44(1):181-186
- 439 23. Aranda A, Matallana E, del Olmo M. *Molecular Wine Microbiology*. Amsterdam, The
440 Netherlands: Elsevier Inc.; 2011:1-31. [https://doi.org/10.1016/B978-0-12-375021-](https://doi.org/10.1016/B978-0-12-375021-1.10001-3)
441 [1.10001-3](https://doi.org/10.1016/B978-0-12-375021-1.10001-3).
- 442 24. Alexandre H, Charpentier C. Biochemical aspects of stuck and sluggish fermentation
443 in grape must. *J Ind Microbiol Biotechnol.* 1998;20(1):20-27.
- 444 25. Jørgensen P, Pedersen JG, Jensen EP, Esbensen KH. On-line batch fermentation
445 process monitoring (NIR)—introducing ‘biological process time’. *J Chemometr.*
446 2004;18(2):81-91